Performance-based evaluation of the response reduction factor for ductile RC frames

CrossMark

Apurba Mondal [a], Siddhartha Ghosh [a,*], G.R. Reddy [b]

[a] *Department of Civil Engineering, Indian Institute of Technology Bombay, Mumbai 400 076, India*
[b] *Reactor Safety Division, Bhabha Atomic Research Centre, Mumbai 400 085, India*

ABSTRACT

Most seismic design codes today include the nonlinear response of a structure implicitly through a 'response reduction/modification factor' (R). This factor allows a designer to use a linear elastic force-based design while accounting for nonlinear behaviour and deformation limits. This research focuses on estimating the actual values of this factor for realistic RC moment frame buildings designed and detailed following the Indian standards for seismic and RC designs and for ductile detailing, and comparing these values with the value suggested in the design code. The primary emphases are in a component-wise computation of R, the consideration of performance-based limits at both member and structure levels, a detailed modelling of the RC section behaviour, and the effects of various analysis and design considerations on R. Values of R are obtained for four realistic designs at two performance levels. The results show that the Indian standard recommends a higher than actual value of R, which is potentially dangerous. This paper also provides other significant conclusions and the limitations of this study.

1. Introduction

Today's seismic design philosophy for buildings, as outlined in different codes and guidelines, such as ASCE7 [1], Eurocode 8 [2], and IS 1893 [3], assumes nonlinear response in selected components and elements when subjected to an earthquake of the design intensity level. However, these codes and guidelines do not explicitly incorporate the inelastic response of a structure in the design methodology. These designs are typically based on the use of elastic force-based analysis procedures rather than displacement-based methods. The equivalent static lateral force method, which has been used from the early days of engineering seismic design, is still the most preferable method to a structural design engineer, because it is conceptually simple and less demanding from a computational point of view. Most of the codes used for seismic design of buildings use the concept of response reduction to implicitly account for the nonlinear response of a structure. In this approach, the design base shear (V_d) is derived by dividing the elastic base shear demand (V_e), which is obtained using an elastic analysis considering the elastic pseudo-acceleration response spectrum (for 5% damping, $S_{a,5}$), by a factor R:

$$V_d = \frac{V_e}{R} = \frac{S_{a,5}W}{R} \tag{1}$$

where W is the seismic weight of the structure. R is termed as the "response reduction factor" in the Indian standard IS 1893 and the "response modification coefficient" in ASCE7. In Eurocode 8 (EC8), the same factor is called the "behaviour factor". There are differences in the way the response reduction factor (R) is specified in different codes for different kinds of structural systems. The objective of the present study is to obtain R for reinforced concrete (RC) regular frame structures designed and detailed as per Indian standards IS 456 [4], IS 1893 [3] and IS 13920 [5]. Existing literature in this area do not provide any specific basis on which a value of 5.0 is assigned for such frames in the Indian standard IS 1893. The present work takes a rational approach in determining this factor for regular RC framed building structures, by considering different acceptable performance limit states. Most of the past research efforts in this area have focused on finding the ductility component of the response reduction factor for single-degree-of-freedom (SDOF) systems considering the local seismicity in different parts of the world. Although some researchers have worked on various components of the response reduction factor in detail, the acceptable limit states considered in these works have been assumed arbitrarily. The work presented in this paper focuses on a component-wise determination of the R factor for RC frames designed and detailed

* Corresponding author. Tel.: +91 2225767309; fax: +91 2225767302.
E-mail addresses: 08404705@iitb.ac.in (A. Mondal), sghosh@civil.iitb.ac.in (S. Ghosh), rssred@barc.gov.in (G.R. Reddy).

as per Indian standard specifications, considering performance limits based on their deformation capacity.

2. Components of R and design standards

Commonly, the response reduction factor is expressed as a function of various parameters of the structural system, such as strength, ductility, damping and redundancy [6–8]:

$$R = R_s R_\mu R_\xi R_R \tag{2}$$

where R_s is the strength factor, R_μ is the ductility factor, R_ξ is the damping factor, and R_R is the redundancy factor. The strength factor (R_s) is a measure of the built-in overstrength in the structural system and is obtained by dividing the maximum/ultimate base shear (V_u) by the design base shear (V_d).

$$R_s = \frac{V_u}{V_d} \tag{3}$$

It should be noted that the strength factor in a structure depends on various factors, such as the safety margins specified in the code that is used to design the structure. Even with the same design code, R_s becomes subjective to the individual designer's choice of a section depending on the demand, because the section provided for a member is never exactly as per the design requirements. For example, the same section will be provided for, say, external columns over two to three stories, although the design requirement usually varies for these. Additionally, the reinforcements provided are typically slightly more than the required due to the availability of discrete rebar sizes. These conservative decisions imparted through a designer's choice adds to R_s. Other parameters which contribute to R_s, are the different partial safety factors. The ductility factor (R_μ) is a measure of the global nonlinear response of a structural system in terms of its plastic deformation capacity. It is measured as the ratio of the base shear considering an elastic response (V_e) to the maximum/ultimate base shear considering an inelastic response (V_u). The different base shear levels used to define these two components (R_s and R_μ) are illustrated in Fig. 1. In the last three decades, significant work has been carried out to establish the ductility factor based on SDOF systems subjected to various types of ground motions. Among these, the works by Newmark and Hall [9], Riddell and Newmark [10], Vidic et al. [11], and Krawinkler and Nassar [12] are significant and are frequently referred to. For a detailed review of research conducted in this area, the reader is requested to refer to the paper by Miranda and Bertero [13]. In this study, the R–μ–T relationships developed by Krawinkler and Nassar [12] are used. These relationships are based on a detailed statistical study

of the response of inelastic SDOF systems (with 5% damping) on rock or stiff soil subjected to strong motion records of the western United States. As per Krawinkler and Nassar [12], the ductility factor can be expressed as

$$R_\mu = [c(\mu - 1) + 1]^{1/c} \tag{4}$$

where μ is the displacement ductility. The parameter c depends on the elastic vibration period (T) and the post- to pre-yield stiffness ratio (α) of the inelastic SDOF system:

$$c = \frac{T^a}{1 + T^a} + \frac{b}{T} \tag{5}$$

a and b are regression parameters, based on α. R_μ values based on Eqs. (4) and (5) are plotted in Fig. 2, which directly provides the ductility factor (R_μ) corresponding to a specific displacement ductility (μ). The ductility capacity ($\mu = \Delta_u/\Delta_y$) is obtained from the bilinearised pushover curve, for the deformation limits corresponding to the selected performance level of failure. The R–μ–T relationship translates this displacement ductility capacity onto the force axis as the R_μ factor. From Fig. 1, it should be understood that the elastic force demand on the system (V_e) can be reduced by the factor R_μ owing to the inelastic displacement capacity (or μ) available with the system. The damping factor (R_ξ) accounts for the effect of "added" viscous damping and is primarily applicable for structures provided with supplemental energy dissipating devices. Without such devices, the damping factor is generally assigned a value equal to 1.0 and is excluded from the determination of the response reduction factor for the purpose of force-based design procedures [6,8]. RC structural systems with multiple lines of lateral load resisting frames are generally in the category of redundant structural systems, as each of the frames is designed and detailed to transfer the earthquake induced inertia forces to the foundation. For these systems, the lateral load is shared by different frames depending on the relative (lateral) stiffness and strength characteristics of each frame. Together, frames aligned in the same direction form a redundant parallel system, and the reliability of the system, theoretically, is more than or equal to each frame's individual reliability. The reliability of the system is higher for structures with multiple lines of frames with uncorrelated characteristics, and the system reliability is reduced to the individual frame's reliability when the resistance parameters are perfectly correlated. Following the conservative suggestion of ASCE7, a redundancy factor $R_R = 1.0$ is used in this study.

The typical value of the response reduction factor specified in different international standards varies depending on the type of structural system as well as the ductility class of the structure un-
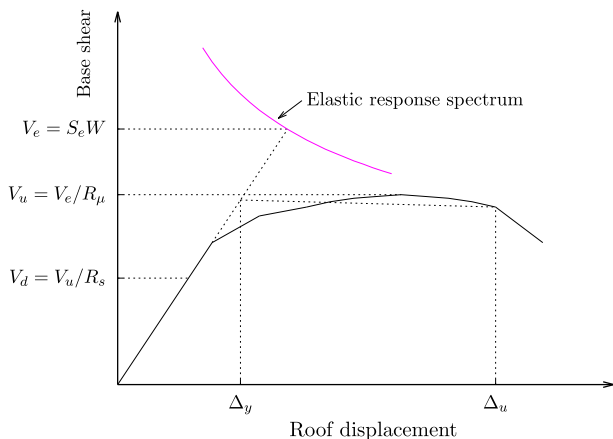
Fig. 1. Sample base shear vs. roof displacement relationship.
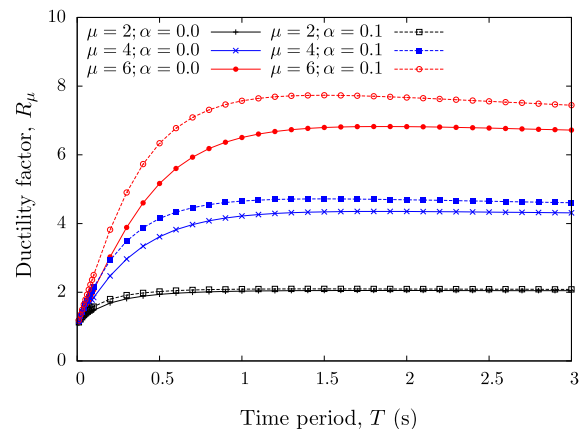
Fig. 2. R–μ–T plot for an inelastic SDOF system.

Table 1
Values of R for RC framed structures, as per IS 1893.

Structural system	R
Ordinary moment resisting frame (OMRF)	3.0
Special moment resisting frame (SMRF)	5.0

Table 2
Values of the 'behaviour factor' for RC framed structures, as per EC8.

Structural system	Behaviour factor
Medium ductility class (DCM)	$3.0V_u/V_y = 3.90$
High ductility class (DCH)	$4.5V_u/V_y = 5.85$

Table 3
Values of R for RC framed structures, as per ASCE7.

Structural system	Response modification coefficient, R	System overstrength factor, Ω_0
Ordinary moment frame	3.0	3.0
Intermediate moment frame	5.0	3.0
Special moment frame	8.0	3.0

der consideration. For regular RC frames, values of R as specified in IS 1893 (Part 1), EC8 and ASCE7 are provided in Tables 1–3, respectively. IS 1893 gives a value of R equal to 3.0 and 5.0 for ordinary and special RC moment resisting frames (OMRF and SMRF). The SMRF needs to follow the ductile detailing requirements of IS 13920. IS 1893 does not explicitly segregate the components of R in terms of ductility and overstrength. Also, it does not specify any reduction in the response reduction factor on account of any irregularity (vertical or plan-irregularity) in the framing system. EC8 gives the behaviour factor (q) for regular RC framed structures for two ductility classes: medium and high (DCM and DCH). The ductility and overstrength components are properly incorporated in the formulation of this factor. The ratio V_u/V_y in Table 2 represents the overstrength component of the behaviour factor, where V_y is the base shear at the first yield. For multistory multibay frames, this ratio is specified in EC8 as 1.30 making the behaviour factor equal to 3.90 and 5.85 for DCM and DCH, respectively. For irregular buildings, the behaviour factor is reduced by 20%. ASCE7 categorises RC frames into three ductility classes (Table 3). It should be noted that although this coefficient is applied for obtaining the design base shear for a structure or framing system, the design of individual members exclude the strength and redundancy components of R. The design member forces are therefore obtained by multiplying the member forces corresponding to the design shear force with the system overstrength (Ω_0). No such specification exists in IS 1893 or EC8.

3. Structural performance limits

The definition of the response reduction factor, R, is integrated to the selected performance limit state of the structure. The Indian standard IS 1893 does not specify the limit state corresponding to which values of R are recommended in this code. However, based on the design philosophy outlined in the initial sections of this seismic design guideline (and comparing with the R values in other codes), it can be safely assumed that these values are based on the ultimate limit state of the structure. Quantitative definition of the ultimate limit state of a structure is also not provided in this code.

Table 4
Deformation limits for different performance levels, as per ATC-40.

	Performance level			
	Immediate occupancy	Damage control	Life safety	Structural stability
Maximum interstorey drift ratio	0.01	0.01–0.02	0.02	$0.33V_i/P_i$

The selection and the definition of a performance limit state to obtain R needs to be looked into in detail, particularly considering similar specifications in newer design standards and guidelines around the world.

Over the last 10–15 years, concepts related to the performance-based seismic design (PBSD) philosophy has gradually entered into the earthquake engineering state of the practice. A PBSD guideline typically provides clear definitions of multiple performance limit states of various types. In PBSD terminology, the limit states are typically known as structural 'performance levels', which in combination with seismic 'hazard levels' define the 'performance objective' for a structure. The performance levels are defined based on the structure type and its intended functions. Different PBSD guidelines, for example ATC-40 [14] or FEMA-356 [15], have provided slightly different definitions (and names) of the performance limit states. Broadly, the performance limits can be grouped into two categories: global/structural limits and local/element/component limits.

The global limits typically include requirements for the vertical load capacity, lateral load resistance and lateral drift. For example, the various performance levels in ATC-40 [14] are specified in terms of the maximum interstorey drift ratio (Table 4). Among these performance levels, the Structural Stability level corresponds to the ultimate limit state of the structure, which can be used for obtaining R (more specifically, R_μ) for a selected structure. One should note that the same performance limit indicating impending collapse is termed as Collapse Prevention in some other documents, such as FEMA-356. For this level, the maximum total interstorey drift ratio in the ith story should not exceed $0.33V_i/P_i$, where V_i is the total lateral shear force demand in the ith storey and P_i is the total gravity load acting at that storey. The local performance levels are typically defined based on the displacement, rotation or acceleration responses of different elements (beams, columns, shear walls, floors, etc.). The limits on the response of structural elements, such as beams and columns, are many times governed by non-structural and component damages as well. For example, Table 5 provides the 'local' deformation limits specified by ATC-40 in terms of plastic hinge rotations of beam elements in a RC moment resisting frame. Table 6 provides similar limiting values of column rotation for different performance levels. These limits are for flexural failures of an element. Therefore, to use these limits, one should ensure that the failure of a member/structure is governed by flexural demands, and shear failure, for example, does not take place before these rotational limits are reached. The

Table 5
Plastic rotation limits for RC beams controlled by flexure, as per ATC-40.

$\frac{\rho-\rho'}{\rho_{bal}}$	Trans. reinf.	$\frac{V}{b_w d\sqrt{f'_c}}$	Immediate occupancy	Life safety	Structural stability
			Plastic rotation limit		
$\leqslant 0$	C	$\leqslant 3$	0.005	0.020	0.025
$\leqslant 0$	C	$\geqslant 6$	0.005	0.010	0.020

C indicates that transverse reinforcement meets the criteria for ductile detailing.

Table 6
Plastic rotation limits for RC columns controlled by flexure, as per ATC-40.

$\frac{P}{A_g f_c'}$	Trans. reinf.	$\frac{V}{b_w d \sqrt{f'_c}}$	Immediate occupancy	Life safety	Structural stability
			Plastic rotation limit		
$\leqslant 0.1$	C	$\leqslant 3$	0.005	0.010	0.020
$\leqslant 0.1$	C	$\geqslant 6$	0.005	0.010	0.015
$\geqslant 0.4$	C	$\leqslant 3$	0.000	0.005	0.015
$\geqslant 0.4$	C	$\geqslant 6$	0.000	0.005	0.010

C indicates that transverse reinforcement meets the criteria for ductile detailing.

capacity design philosophy, which is incorporated in most seismic design codes today, ensures a preferred failure hierarchy. The shear detailing provisions specified in IS 13920 ensures that shear failure does not initiate before the formation flexural plastic hinges at member ends. On the basis of these background information, it is decided to consider an ultimate limit state based on flexural failure at both local and global levels in this paper. Due to the lack of such detailed definition of any ultimate limit state in the Indian standard IS 1893, the Structural Stability performance level of ATC-40 is used here, both at the structure level and at the member levels. In addition, actual member plastic rotation capacities, for individual members, are also considered in obtaining R for real RC frames.

4. Description of the structural systems considered

The structural systems considered for this study are four typical symmetric-in-plan RC frame structures having two-, four-, eight- and 12-storied configurations, intended for a regular office building in the seismic zone IV as per IS 1893 [3]. The seismic demands on these buildings are calculated following IS 1893. The RC design for these buildings are based on IS 456 guidelines [4] and the (seismic) ductile detailing of the RC sections are based on IS 13920 provisions [5]. The study building is assumed to be located in zone IV, which is the second most seismically intensive zone covering a large part of the country including the national capital New Delhi and several other sate capitals. The design base shear for a building is derived as:

$$V_d = \frac{ZIS_a}{2Rg} W \tag{6}$$

where Z denotes the zone factor (= 0.24 for zone IV), I is the structure's importance factor (= 1 for these buildings), R = 5.0 for ductile or 'special' moment resisting frames (SMRF), S_a is the spectral acceleration, and W is the seismic weight of the structure. All study structures have the same plan arrangement with four numbers of bays (6.0 m each) in both directions as shown in Fig. 3. The floor to floor height is 4.0 m for all the storeys and the depth of foundation is 3.0 m. A typical elevation (for the 4-storied frame) is shown in Fig. 4. These moment resisting frame structures of different heights are selected to typically represent "short", "medium" and "long" period structures. Further details on these planar frames, such as total height (from the foundation level), fundamental period, total seismic weight, and design base shear, are provided in Table 7. Fig. 5 shows the fundamental periods of these four frames on the 5% damping pseudo-acceleration design spectrum specified in IS 1893 for a 'medium' soil condition in Zone IV [3]. The fundamental periods of the structures, presented in Table 7, are calculated based on the empirical formula recommended in IS 1893. The RC frames are designed with M25 grade concrete (having 28 days characteristic cube strength of 25 MPa) and Fe415 grade reinforcements (having a characteristic yield strength of 415 MPa) [4].
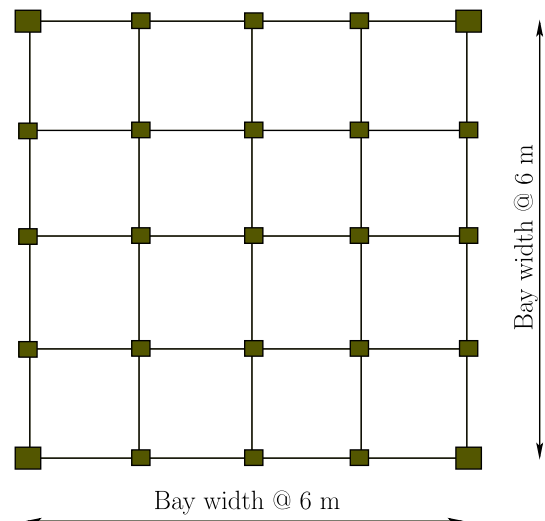
Fig. 3. Structural arrangement of the four buildings in plan.
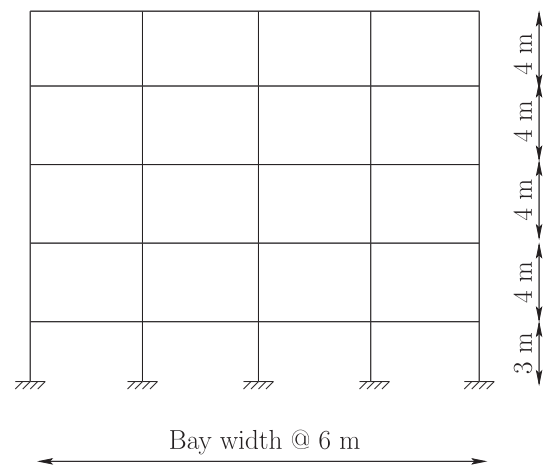
Fig. 4. Elevation of the four-story RC frame structure.

Table 7
Details of the RC frames considered for the case study

Frame	Height (m)	T_d (s)	W (kN)	$A_h = V_d/W$	V_d (kN)
2-Storey	11.0	0.453	4650	0.0600	279
4-Storey	19.0	0.683	7770	0.0478	371
8-Storey	35.0	1.08	13800	0.0302	416
12-Storey	51.0	1.43	19800	0.0228	451

As mentioned earlier, the selected structural design for a building is not a unique solution available for the demands calculated. Based on the same demand, different designers may select different design solutions. The RC design solutions selected for these buildings are based on common practices adopted by design engineers. For example, in a planar frame, all the internal columns in a storey are chosen to have the same section and similarly the beams in a specific floor. The column sections remain the same over two to three storeys depending on the building height. The Indian standards do not specifically enforce a strong-column-weak-beam (SCWB) behaviour. However, considering the practice followed in most countries, the strong-column-weak-beam requirement (in terms of beam and column moment capacities) is considered in these designs. The RC section details ensuring the strong-column-weak-beam behaviour are
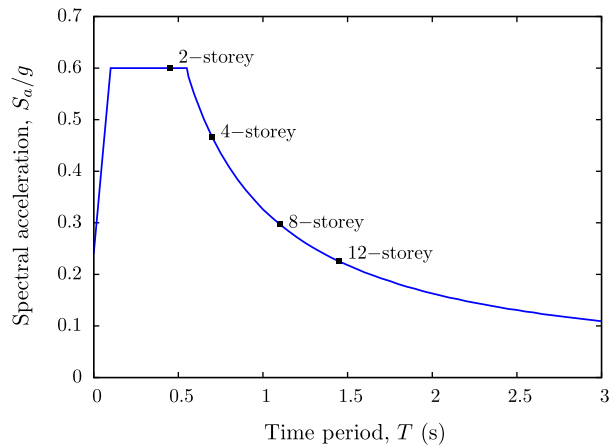
Fig. 5. 5% damping response spectrum for 'medium' soil in zone IV, as per IS 1893.

provided in Table 8. An alternative set of designs are also obtained without considering the strong-column-weak-beam requirement in selecting the sections, which is discussed in detail in Section 7.3. The response reduction factor (R) is obtained for both sets of designs.

5. Modelling of RC members

Estimation of R values of these study frames depends significantly on how well the nonlinear behaviour of these frames are represented in analyses. Since R values are estimated on the basis of nonlinear static pushover analyses, the focus of the modelling scheme employed here is to capture the nonlinear static behaviour of the RC frame members. A few critical aspects of the modelling scheme adopted in this work are described in this section. The non-linear behaviour of the frame depends primarily of the moment–rotation behaviour of its members, which in turn depends on the moment–curvature characteristics of the plastic hinge section and the length of the plastic hinge. These two parameters also define the 'component' level performance limit in terms of the plastic rotation capacity. In addition to these two aspects, the other important aspect that is discussed in this section is the initial stiffness of a member which affects the force-deformation relation in the 'linear elastic' zone.

5.1. Moment–curvature characteristics of RC sections

The moment–curvature (M–ϕ) characteristics of various RC sections are developed using the widely used Kent and Park model [16], which considers the confinement effect of the (closed) transverse reinforcements. Various other analytical models for this, that are frequently referred to in literature, are those proposed by Mander et al. [17], Baker and Amarakone [18], Roy and Sozen [19], Soliman and Yu [20], Sargin et al. [21], Sheikh and Uzumeri [22], and Saatcioglu and Razvi [23]. Based on the results of experiments conducted on a large number of beam-column joints of different dimensions, Sharma et al. [24] concluded that response estimations using the Kent and Park model closely matched the experimental results in the Indian scenario. The ductile design provisions of IS 13920 require that transverse reinforcements in beams and columns should be able to confine the concrete core. Considering this, the Kent and Park model for confined concrete is used for the concrete within the stirrups, and unconfined concrete characteristics, following again the Kent and Park guidelines, are assigned to the cover concrete. Spalling of the concrete cover is also modelled in case the strain outside the confined core exceeds the ultimate compressive strain of unconfined concrete. Priestley [25] prescribed an ultimate concrete strain (in compression) for unconfined concrete, $\epsilon_{cu} = 0.005$, which is adopted in this work. The ultimate compressive strain of concrete confined by transverse reinforcements (ϵ_{cc}) as defined in ATC-40 is adopted in this work to develop the M–ϕ characteristics of plastic hinge sections:

$$\epsilon_{cc} = 0.005 + 0.1 \frac{\rho_s f_y}{f'_c} \leqslant 0.02 \tag{7}$$

In order to avoid the buckling of longitudinal reinforcement bars in between two successive transverse reinforcement hoops, the limiting value of ϵ_{cc} is restricted to 0.02. Other researchers, for example, Priestley [25], also proposed similar expressions for the ultimate compressive strain of confined concrete. A typical M–ϕ curve for a RC beam section under hogging (tension at top) moments for the four-storey frame is shown in Fig. 6. Considering the presence of rigid floor diaphragms, the effects of axial force on a beam's M–ϕ behaviour are disregarded. However, these effects are included while obtaining the M–ϕ relation for the column sections. Fig. 7 shows a typical M–ϕ plot for an exterior column section of the four-storey frame, for different levels of axial force P (normalised to its axial force capacity, P_{uz}). It is observed that there is a drop in the M–ϕ curves for both beam and column sections after the peak moment capacity is reached. This is on account of the spalling of the

Table 8
RC section details for the study frames (with the SCWB design criterion).

Frame	Members	Floors	Width (mm)	Depth (mm)	Reinforcement details
2-Storey	Beams	1–2	250	500	$[3 - 25\Phi + 2 - 20\Phi]$(top) + $[2 - 25\Phi + 1 - 20\Phi]$ (bottom)
	Columns	1–2	450	450	$8 - 25\Phi$ (uniformly distributed)
4-Storey	Beams	1–4	300	600	$6 - 25\Phi$ (top) + $3 - 25\Phi$ (bottom)
	Columns	1–4	500	500	$12 - 25\Phi$ (uniformly distributed)
8-Storey	Beams	1–4	300	600	$6 - 25\Phi$ (top) + $3 - 25\Phi$ (bottom)
	Columns	1–4	600	600	$12 - 25\Phi$ (uniformly distributed)
	Beams	5–8	300	600	$6 - 25\Phi$ (top) + $3 - 25\Phi$ (bottom)
	Columns	5–8	500	500	$12 - 25\Phi$ (uniformly distributed)
12-Storey	Beams	1–4	300	650	$6 - 25\Phi$ (top) + $3 - 25\Phi$ (bottom)
	Columns	1–4	750	750	$12 - 25\Phi$ (uniformly distributed)
	Beams	5–8	300	600	$6 - 25\Phi$ (top) + $3 - 25\Phi$ (bottom)
	Columns	5–8	600	600	$12 - 25\Phi$ (uniformly distributed)
	Beams	8–12	250	550	$6 - 25\Phi$ (top) + $3 - 25\Phi$ (bottom)
	Columns	8–12	500	500	$12 - 25\Phi$ (uniformly distributed)

Φ is the diameter of a rebar.
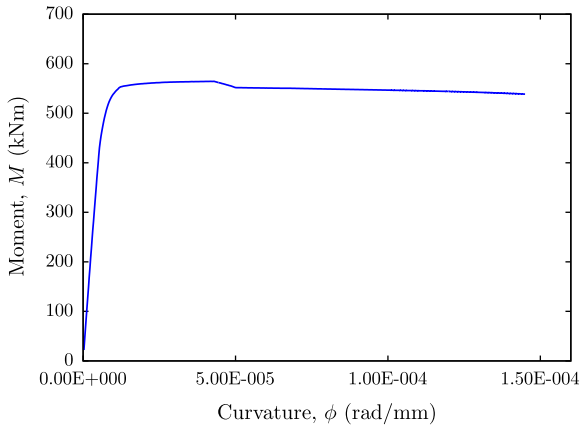
Fig. 6. Sample M–ϕ characteristics of a beam section of the four-storey frame under 'hogging' bending moment.
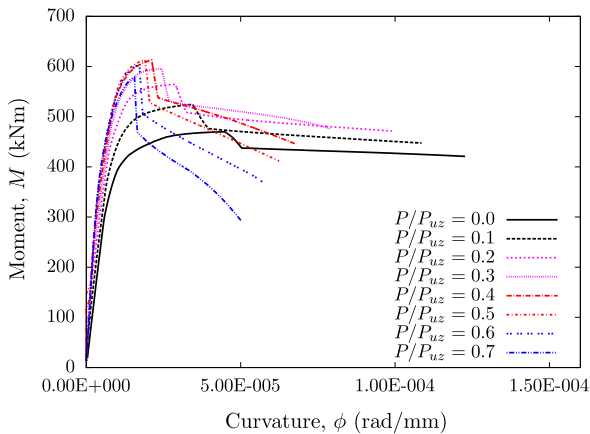
Fig. 7. Sample M-ϕ characteristics of a column (external) section of the four-storey frame.

concrete cover when the strain in concrete in that region exceeds the ultimate strain for unconfined concrete ($\epsilon_{cu} = 0.005$). This is more prominent for column sections than beam sections and this drop becomes more significant as (P/P_{uz}) is increased.

5.2. Plastic hinge characteristics

The plastic rotation capacity (θ_p) in a reinforced concrete member depends on the ultimate curvature (ϕ_u) and the yield curvature (ϕ_y) of the section and the length of the plastic hinge region (L_p):

$$\theta_p = (\phi_u - \phi_y)L_p \qquad (8)$$

Park and Paulay [26] reported that various researchers had proposed different empirical models to predict the length of a plastic hinge. One of the most widely used models for L_p is that proposed by Priestley [25]:

$$L_p = 0.08L + 0.022f_{ya}d_{bl} \qquad (9)$$

where L is the distance from the critical section to the point of contraflexure, f_{ya} is the yield strength (in MPa) of longitudinal bars having a diameter d_{bl}. For a moment-resisting frame, where lateral loads (for example, seismic) are predominant, the point of contraflexure typically occurs close to the mid-span of a member. The plastic rotation capacities of frame members of the four study structures are computed using Equations (8) and (9), assuming the points of contraflexure to be at the mid-span of members. Sample plastic rotation capacities computed for some typical members of the 12-storey frame (for which Table 8 provides the section details) are given in Table 9. These capacities are computed for purely flexural conditions, without the effects of any axial load. The plastic rotation capacities of the column elements for different (normalised) axial load levels are provided in Table 10. As suggested by many previous researchers for this type of framed structures, the lumped plasticity model, with plastic hinge formation possibility at both ends of a member, is used for nonlinear static pushover analyses.

5.3. Initial stiffness of RC members

Appropriate modelling of the initial stiffness of RC beams and columns is one of the important aspects in the performance evaluation of reinforced concrete frames. The initial stiffness of members significantly affects the yield displacement of a frame structure. Consequently, the displacement ductility (μ), which is the ratio of the ultimate to the yield displacement, is also greatly affected by the initial stiffness of members adopted in the nonlinear static analysis. The stiffness of a reinforced concrete section may be determined as a function of its material properties, reinforcement quantities, and induced stress and deformation levels. For a primarily flexural member, the effective stiffness can be computed by considering (a) the variation of bending moment along its length and (b) the 'cracked' moment of inertia of the transformed section. Various other parameters, that affect the force deformation characteristics of a cracked concrete section, are the deformation due to shear cracking, partial reinforcement slip from adjacent joints, effect of aggregate interlock, dowel action of reinforcement bars, tension stiffening, etc. The exact estimation of initial stiffness of each individual member incorporating all of these effects becomes impractical due to the complexity involved in modelling and the increased demand on computation. Considering this, it is suggested in both ATC-40 [14] and FEMA-356 [15] to use the following values for initial stiffness of RC members: $0.5E_cI_g$, $0.7E_cI_g$

Table 9
Plastic rotation capacities of the frame sections of 12-storey frame structure.

Member	Action	Size (mm)	Clear span (mm)	L_p (mm)	ϕ_y (rad/mm)	ϕ_u (rad/mm)	θ_p (rad)
Beam	+M	300 × 650	5250	438	8.93E−06	2.48E−04	0.105
Beam	−M	300 × 650	5250	438	1.08E−05	1.00E−04	0.0391
Beam	+M	300 × 600	5400	444	9.56E−06	2.48E−04	0.106
Beam	−M	300 × 600	5400	444	1.22E−05	1.01E−04	0.0392
Beam	+M	250 × 550	5500	448	1.13E−05	2.47E−04	0.106
Beam	−M	250 × 550	5500	448	1.48E−05	8.41E−05	0.0311
Column	±M	750 × 750	3350	362	7.57E−06	1.28E−04	0.0435
Column	±M	600 × 600	3400	364	1.06E−05	1.25E−04	0.0418
Column	±M	500 × 500	3450	366	1.40E−05	1.23E−04	0.0398

+M indicates 'sagging' moment (causing tension at the bottom of a beam). The longitudinal bar is of 25 mm diameter and the yield strength is 415 MPa. θ_p for column sections are based only on flexural actions.

Table 10
Axial load effects on column plastic rotation capacities for the 12-storey frame structure.

Axial load P_u/P_{uz}	Plastic rotation capacity, θ_p (rad)		
	Column	Column	Column
	(750×750)	(600×600)	(500×500)
0.0	0.0435	0.0418	0.0398
0.1	0.0249	0.0272	0.0343
0.2	0.0178	0.0236	0.0304
0.3	0.0148	0.0196	0.0224
0.4	0.0115	0.0140	0.0174
0.5	0.00838	0.0111	0.0159
0.6	0.00657	0.0101	0.0146
0.7	0.00598	0.00911	0.0126
0.8	0.00538	0.00822	0.0122
0.9	0.00494	0.00791	0.0118

and $0.5E_cI_g$ for beams, columns under compression, and columns under tension, respectively. E_c is the modulus of elasticity of concrete and I_g is the moment of inertia of the 'gross section'. Since a column may be subjected to both compression and tension in alternate cycles during earthquakes, an average value of $0.6E_cI_g$ is adopted as the initial stiffness for all column elements, following ATC-40's suggestion.

6. Nonlinear static pushover analysis of RC frames

Nonlinear static pushover analyses (NSPA) of the four study frames are performed to estimate their overstrength and global ductility capacity, which are required for computing R for each frame. The equivalent lateral force distribution adopted for this pushover analysis is as suggested in IS 1893:

$$Q_i = V_d \frac{W_i h_i^2}{\sum\limits_{i=1}^{n} W_i h_i^2} \qquad (10)$$

where Q_i is the equivalent lateral force on the ith floor, W_i the seismic weight of the ith floor, h_i the height up to the ith floor, and n is the total number of storeys. More complex, vibration mode/period-dependent distributions have been suggested in other codes, such as ASCE7; however, the distribution as per IS 1893 is used in this study considering its overwhelming use in India. The effect of adopting other lateral load distributions in NSPA on the R factor is discussed in detail in Section 7.6. Owing to the rigid floor diaphragm in every floor and the symmetric-in-plan configuration avoiding any torsional motion, only a two-dimensional pushover analysis of a single frame is performed for these evaluations.

The NSPA are performed using the DRAIN-2DX analysis software [27]. The intermediate frames having maximum gravity load effects are considered for the pushover analysis. All beam and column members are modelled using the 'plastic hinge beam column element (Type 02)' available in DRAIN-2DX. For beam members, the axial load effects are ignored considering the rigid floor diaphragm effect. For column members, the effect of axial loads on plastic hinges are considered using a P–M interaction diagram for each different RC section. A typical P–M interaction plot for the 500×500 column section is shown in Fig. 8. No shear hinge formation is considered in these analyses, as the various design and detailing provisions specified in IS 13920 eliminate the possibility of such a failure. The joint panel zones are assumed to be rigid and strong enough to avoid any premature failure before forming a mechanism by the failure of other members, following again the capacity design concepts adopted in IS 13920.

The design gravity loads are applied before applying the incremental lateral forces. The gravity loads are applied as distributed
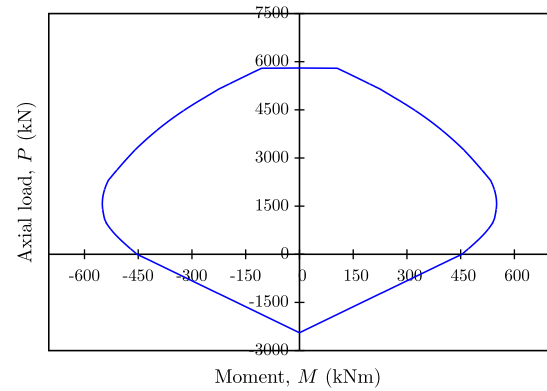
Fig. 8. Sample P–M interaction for an external column section of the four-storey frame.

element loads based on yield line theory and concentrated loads from secondary beams. First, a static analysis is performed for the full gravity load in a single step. The state of the structure from this analysis is saved and subsequently the static pushover analysis is conducted starting from this state of the structure. For the nonlinear static analysis, both the load control and the displacement control strategies are adopted. The analysis is load controlled up to the first yield and displacement controlled thereafter. The inclusion of P–Δ effects changes the lateral force-deformation behaviour of a frame. Section 7.5 discusses in detail the effects of including (and, of not including) geometric nonlinearity in NSPA on the computed R values. The output of a nonlinear static analysis is generally presented in the form of a 'pushover curve', which is typically the base shear vs. roof displacement plot. Pushover curves obtained from NSPA performed on the two-, four-, eight- and 12-storey frames are shown in Figs. 9–12, respectively. The interstorey drift ratio values are checked at every load/displacement increment against the performance limits defined. Similarly at the member level, the plastic rotations for individual components are also checked against the respective limits based on the induced load levels. The performance level is marked on the pushover curve, when for the first time any of these limits is reached.

7. Computation of R for the study frames

As mentioned earlier in Section 3, two performance limits are considered in the computation of R for the study frames. The first one (*Performance Limit 1* or PL1) corresponds to the Structural Stability limit state defined in ATC-40, which is exactly the same or
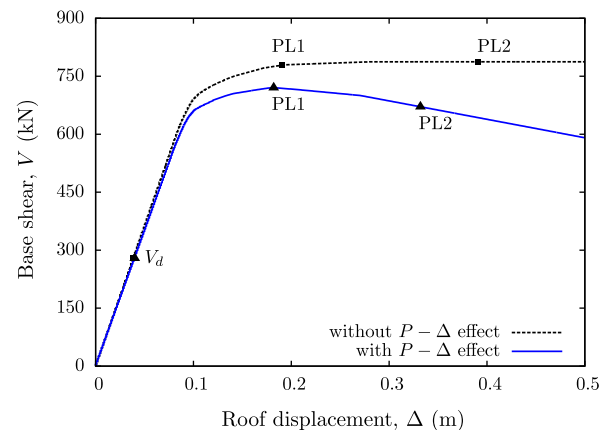
Fig. 9. Pushover curves for the two-storey frame.
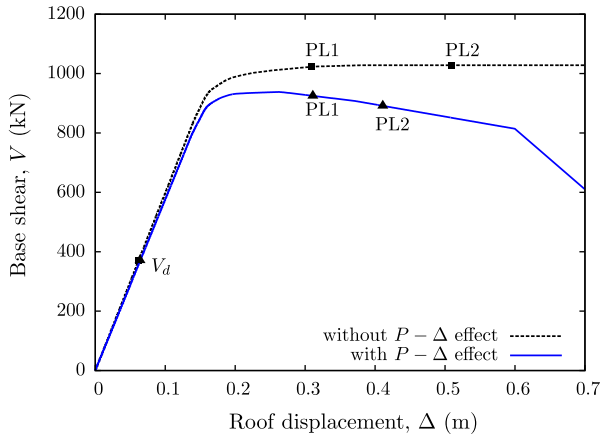
Fig. 10. Pushover curves for the four-storey frame.
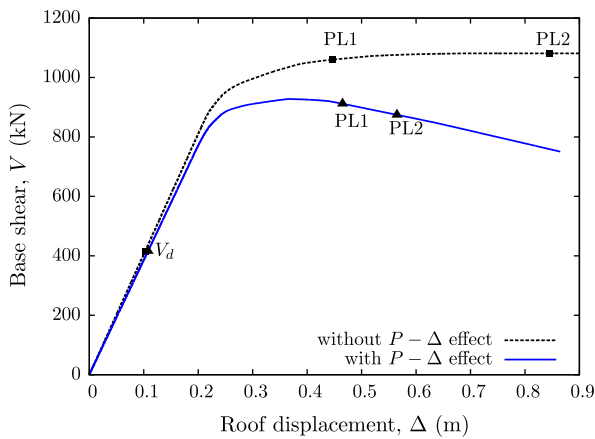
Fig. 11. Pushover curves for the eight-storey frame.
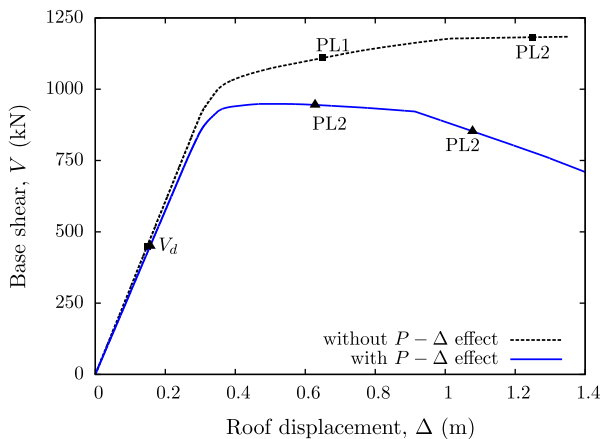
Fig. 12. Pushover curves for the 12-storey frame.

very close to the ultimate limit states defined in subsequent seismic design/assessment guidelines, such as FEMA-356. This limit state is defined both at the storey level (in terms of the maximum interstorey drift ratio) and at the member level (in terms of the allowable plastic hinge rotation at member ends). The second limit state (*Performance Limit 2* or PL2) is based on plastic hinge rotation capacities that are obtained for each individual member depending on its cross-section geometry, as discussed in Section 5.2.

In order to compute the different components of the response reduction factor, various parameters, such as roof displacement, base shear, interstorey drift ratio, and member plastic rotation – pertaining to both the yield and the ultimate limit states of a structure – are obtained from the NSPA. The limit state of 'yield' of a structure, in this paper, is based on a bilinearisation of the base shear vs. roof displacement ('pushover') plot, considering equal areas under the actual and the approximating curves. A similar scheme of bilinearisation was adopted in many previous studies on performance-based seismic design [6,28,29]. This section first provides the results of computing the R factor considering both PL1 and PL2, and then discusses the effect of several considerations in the methodology adopted on the computed values of R.

7.1. Computation of R for PL1

The global performance limit for PL1 is defined by a maximum interstorey drift ratio of $0.33V_i/P_i$ (Table 4). For the four study structures, where the maximum V_i (at the base) is around 6% of the P_i, this limit is found to be 0.02. At the component level, based on the sectional configuration as well as the induced load level (normalised with respect to respective section capacities), the plastic rotation limits of individual member is derived from the values given in Tables 5 and 6, for beam and column elements, respectively. These three quantities defining both the structure level and component level limits are monitored continuously at each load/displacement increment during the NSPA, and the analysis is terminated when one of the limit states is reached. Figs. 9–12 present the pushover plots for the study frames for both including and excluding P–$\varDelta$ effects in the analysis. Points marked 'PL1' in these base shear vs. roof displacements curves mark the first instants of reaching a PL1 limit state, as described earlier. PL1 can thus be due to reaching the specified maximum interstorey drift ratio or the plastic rotation at member ends. For each of the study frames, Table 11 shows which of these limit states is governing. Parameters necessary for the computation of R – the maximum base shear up to the specific performance limit (V_u), ultimate roof displacement ($\varDelta_u$), yield base shear (V_y) and the yield roof displacement ($\varDelta_y$) – are obtained from the pushover plots (or from their bilinear approximations). Table 11 also presents the values of these parameters for each study frame, along with the ductility ratio (μ) and the overstrength (Ω) derived from these parameters. The response reduction factor (R) computed on the basis of these parameters are shown in Table 12 for the four frames, along with a component-wise break-up for R. A value of $R_R = 1.0$ is adopted as in these calculations, based on ASCE7's recommendation for similar parallel load-resisting frames.

The R values range from 4.23 to 4.96 for the four frames considered, and are all lesser than the IS 1893 specified value of R (= 5.0) for ductile/'special' RC moment frames. The range of R values can be considered to be narrow, indicating a consistent storey-level performance for all frames (note that the failure is governed by an interstorey drift ratio based limit state for all frames). The taller frames among the four studied show lower R values. Component-wise, the shorter frames (two-storey and four-storey) have more overstrength and R_s, but slightly less ductility and R_μ compared to the taller frames.

7.2. Computation of R for PL2

It is observed that for the study frames, where maximum the design base shear is around 6.0% of the seismic weight, the interstorey drift ratio based limits become the same for both the 'Structural Stability' and 'Life Safety' performance levels of ATC-40. Therefore, the PL1 limits adopted in this work may be argued to be conservative, and not representing the 'ultimate' limit state

Table 11
Pushover parameters for PL1, considering P–Δ effects.

Frame	V_d (kN)	V_u (kN)	Δ_y (m)	Δ_u (m)	Limiting parameter	$\mu = \Delta_u/\Delta_y$	$\Omega = V_u/V_d$
2-storey	279	720	0.0957	0.182	IDR, storey 1	1.90	2.58
4-storey	371	938	0.160	0.310	IDR, storey 1	1.93	2.53
8-storey	416	928	0.231	0.460	IDR, storey 2	1.99	2.23
12-storey	451	949	0.314	0.617	IDR, storey 1	1.97	2.11

IDR stands for interstorey drift ratio.

Table 12
Components of R based on PL1 and PL2 (considering P–Δ effects).

Frame	Based on PL1				Based on PL2			
	R_s	R_μ	R_R	R	R_s	R_μ	R_R	R
2-storey	2.58	1.92	1.00	4.96	2.58	3.20	1.00	8.48
4-storey	2.53	1.97	1.00	4.97	2.53	2.59	1.00	6.54
8-storey	2.23	2.04	1.00	4.56	2.23	2.45	1.00	5.46
12-storey	2.11	2.01	1.00	4.23	2.11	3.37	1.00	7.09

for these structures [30]. Considering this, the actual plastic rotation capacities of member sections – based on their cross-sectional properties including reinforcements – are considered for defining the 'ultimate' limit state in PL2. Thus, PL2 remains a member level limit state while in PL1 both structure and member level failures are considered.

The plastic rotation capacities of beam and column sections are obtained on the basis of their moment–curvature characteristics as described in Section 5.2. Similar to PL1, the nonlinear static pushover analyses are performed on the four frames and all the necessary responses are monitored till the plastic rotation capacity in any member is reached. Figs. 9–12 also mark on the pushover plots when PL2 is reached, for both with and without P–Δ effects. Table 13 provides the important parameters obtained from these pushover plots, including the ductility and the overstrength. Similar to Table 11, this table marks the location where the limiting plastic rotation for PL2 is reached first.

The pushover plots clearly show that, for all frames, PL2 is reached after PL1 (that is, for a larger roof displacement). Based on the pushover plots (and their bilinearisation), V_u values come out to be the same as those for PL1. Since V_d values do not change, Ω values are also the same as in PL1. There are very minor variations from PL1 values for Δ_y values. Δ_u values for PL2, as mentioned earlier, are larger than corresponding PL1 values. and so are the ductility values for each frame. Among the various components of R (presented in Table 12), R_s remains the same as in PL1, while R_μ values come out to be higher, which finally results in higher R factors overall. For PL2, R ranges from 5.46 to 8.48. This increased variation in R signifies that the four designs are not very consistent in terms of a member rotation based performance level.

7.3. Effects of not adhering to the strong-column-weak-beam criterion

It may be noted that thestrong-column-weak-beam (SCWB) design is a desirable but not mandatory requirement as far as the Indian seismic design standard is concerned. Therefore, it is possible

to meet all the (Indian) codal requirements for these four designs without looking at the 'flexural' SCWB criterion defined in terms of relative moment capacities of members at each beam-column joint. Alternative designs for the four study buildings are thus obtained without looking at the SCWB criterion. The section details for these alternative designs are provided in Table 14. It is observed that in most of these cases, the design requirement for elements – considering all the code specified load combinations for gravity and seismic loads – requires member sizes in such a way that the SCWB criterion is automatically satisfied. However in few other cases, particularly in the upper stories, the design requirements are met with a weak-column-strong-beam configuration. This happens for the internal columns in the upper stories of the four-, eight-, and 12-storey frames. The response reduction factor for these designs are computed for both PL1 and PL2, and are presented in Table 15. For PL1, values of R remain the same as those for the original designs considering the SCWB criterion, which signifies that the SCWB and non-SCWB designs do not differ from a maximum interstorey drift demand perspective. Even for PL2, the values of R are not significantly affected by the SCWB to non-SCWB shift in the design.

7.4. Sensitivity to the fundamental period used in computing R

An accurate estimation of the fundamental period of vibration (T_1) of a structure is important in the determination of its R factor. The computation of the design base shear depends on T_1. T_1 also determines the ductility factor (R_μ) based on the displacement ductility, μ. Standard design practices typically use code-recommended empirical equations for estimating the design base shear. The same practice is followed here in calculating V_d for the four study frames. However, to obtain R_μ from the R–μ–T relations developed by Krawinkler and Nassar [12], T_1 is based on an eigensolution of the structural model used in DRAIN-2DX. The accuracy of the estimation based on eigensolution depends on how close the structural model is to the actual structure, particularly in modelling the mass and stiffness properties. Considering the standard modelling practices adopted in this work, T_1 based on the eigensolution can be assumed to be sufficiently accurate for computing R. In this section, we check the effects of using T_1 based on the code-recommended empirical equation in the R–μ–T relations. IS 1893 [3] suggests an approximate formula for estimating T_1 of a RC moment framed building without brick infill panels:

$$T_1 = 0.075h^{0.75} \tag{11}$$

Table 13
Pushover parameters for PL2, considering P–Δ effects.

Frame	V_d (kN)	V_u (kN)	Δ_y (m)	Δ_u (m)	Limiting parameter	$\mu = \Delta_u/\Delta_y$	$\Omega = V_u/V_d$
2-storey	279	720	0.104	0.332	θ_p, ground column	3.20	2.58
4-storey	371	938	0.164	0.409	θ_p, storey 1 col.	2.50	2.53
8-storey	416	928	0.237	0.560	θ_p, storey 1 col.	2.36	2.23
12-storey	451	949	0.336	1.07	θ_p, storey 1 col.	3.18	2.11

Table 14
RC section details for the study frames (without the SCWB design criterion).

Frame	Members	Floors	Width (mm)	Depth (mm)	Reinforcement details
2-storey	Beams	1–2	250	500	$[3-25\Phi+2-20\Phi]$ (top) + $[2-25\Phi+1-20\Phi]$ (bottom)
	Interior columns	1–2	450	450	$8-25\Phi$ (uniformly distributed)
	Exterior columns	1–2	450	450	$8-25\Phi$ (uniformly distributed)
4-storey	Beams	1–4	300	600	$6-25\Phi$ (top) + $3-25\Phi$ (bottom)
	Interior columns	1–4	500	500	$4-28\Phi+4-25\Phi$ (uniformly distributed)
	Exterior columns	1–4	500	500	$12-25\Phi$ (uniformly distributed)
8-storey	Beams	1–4	300	600	$6-25\Phi$ (top) + $3-25\Phi$ (bottom)
	Interior columns	1–4	600	600	$12-25\Phi$ (uniformly distributed)
	Exterior columns	1–4	600	600	$12-25\Phi$ (uniformly distributed)
	Beams	5–8	300	600	$6-25\Phi$ (top) + $3-25\Phi$ (bottom)
	Interior columns	5–8	500	500	$8-25\Phi$ (uniformly distributed)
	Exterior columns	5–8	500	500	$12-25\Phi$ (uniformly distributed)
12-storey	Beams	1–4	300	650	$6-25\Phi$ (top) + $3-25\Phi$ (bottom)
	Interior columns	1–4	750	750	$12-25\Phi$ (uniformly distributed)
	Exterior columns	1–4	750	750	$12-25\Phi$ (uniformly distributed)
	Beams	5–8	300	600	$6-25\Phi$ (top) + $3-25\Phi$ (bottom)
	Interior columns	5–8	600	600	$12-25\Phi$ (uniformly distributed)
	Exterior columns	5–8	600	600	$12-25\Phi$ (uniformly distributed)
	Beams	8–12	250	550	$6-25\Phi$ (top) + $3-25\Phi$ (bottom)
	Interior columns	8–12	500	500	$8-25\Phi$ (uniformly distributed)
	Exterior columns	8–12	500	500	$12-25\Phi$ (uniformly distributed)

Φ is the diameter of a rebar.

Table 15
Components of R, without the SCWB design criterion.

Frame	Based on PL1				Based on PL2			
	R_s	R_μ	R_R	R	R_s	R_μ	R_R	R
2-storey	2.58	1.92	1.00	4.96	2.58	3.20	1.00	8.48
4-storey	2.33	2.13	1.00	4.97	2.33	2.79	1.00	6.52
8-storey	2.20	2.05	1.00	4.53	2.20	2.67	1.00	5.88
12-storey	2.11	2.01	1.00	4.23	2.11	3.52	1.00	7.41

where T_1 is measured in seconds and h is the height of the building in metres. Other seismic design standards also suggest similar empirical equations for T_1, and these equations typically give a 'conservative' value, such that V_d is estimated on the higher side.

Fundamental time periods for the four frames based on this equation, along with the ones based on eigensolution, are provided in Table 16. The code-based T_1 values are in the range of 50.0–60.0% of the T_1 based on the eigensolution. Table 16 also provides the values of R (for both PL1 and PL2) based on the code-based T_1 values. The effect of the reduction in T_1 on R (R_μ, to be more specific) is observed only for the two- and four-storey frames. For these two frames R_μ changes, while there is (almost) no change in R_μ for the other two frames. Fig. 2 explains this phenomenon. For the two- and four-storey frames, the reduction in R is more in PL2 than in PL1. In this context, it should also be mentioned that there is an elongation of T_1 when the structure goes into its inelastic behaviour. This elongation may cause an increase in R_μ, only if the elastic T_1 was in the 'constant acceleration' range (typically, below 0.5–0.7 s).

7.5. Effects of not including P–Δ effects in analyses

The nonlinear static pushover analyses, used so far for obtaining values of R for two performance levels, included P–$\varDelta$ effects in order to reflect the structural behaviour as accurately as possible. As an academic exercise, we check here if the inclusion or exclusion of these effects is important at the selected performance levels (PL1 and PL2) for the four study frame. Pushover plots for these frames without the global P–$\varDelta$ effects are shown in Figs. 9–12 along with 'with P–$\varDelta$' plots, for an easy comparison. As expected, the 'without P–$\varDelta$' plots show a monotonically non-decreasing (in terms of the base shear) curve, unlike the 'with P–$\varDelta$' plots which show a downward curve after attaining a maximum base shear (V_u). Table 17 presents the results of these 'without P–$\varDelta$' analyses in terms of R and its components. For PL1, there is an increase in R_s and the final R values range between 4.86 and 5.50, which are around the IS 1893 specified value of 5.0. However for PL2, there is a significant increase in R_μ, along with some increase in R_s. This causes a very visible rise in R values for all frames, to the range of 8.79–10.9. The effects P–$\varDelta$ are more significant on θ_p at the member level than on interstorey drift ratios, which causes a significant difference in R_μ values between with and without P–$\varDelta$ analyses.

7.6. Effects of the lateral load distribution pattern used in NSPA

Values of R computed so far are based on pushover analyses considering the quadratic lateral distribution pattern suggested in IS 1893 (Eq. (10)). It should be worthwhile to check if these value change (and if they do, to what extent they change) if we considered a different lateral load distribution in the NSPA. ASCE7 [1]

Table 16
Components of R based on the code-recommended fundamental period.

Frame	Fundamental period, T_1 (s)		Based on PL1				Based on PL2			
	Code	Eigensolution	R_s	R_μ	R_R	R	R_s	R_μ	R_R	R
2-storey	0.453	0.884	2.58	1.83	1.00	4.73	2.58	2.89	1.00	7.46
4-storey	0.683	1.16	2.53	1.92	1.00	4.86	2.53	2.48	1.00	6.28
8-storey	1.08	1.97	2.23	2.03	1.00	4.53	2.23	2.42	1.00	5.41
12-storey	1.43	2.60	2.11	2.01	1.00	4.24	2.11	3.37	1.00	7.09

Table 17
Components of R, without the P–Δ effects.

Frame	Based on PL1				Based on PL2			
	R_s	R_μ	R_R	R	R_s	R_μ	R_R	R
2-storey	2.79	1.97	1.00	5.50	2.82	3.86	1.00	10.9
4-storey	2.76	1.93	1.00	5.32	2.77	3.17	1.00	8.79
8-storey	2.55	1.91	1.00	4.86	2.60	3.55	1.00	9.22
12-storey	2.46	1.98	1.00	4.88	2.62	3.77	1.00	9.89

suggested a distribution based on the fundamental vibration period (T_1):

$$Q_i = V_d \frac{W_i h_i^k}{\sum\limits_{i=1}^{n} W_i h_i^k} \tag{12}$$

where k is an exponent related to T_1: for $T_1 \leqslant 0.5$ s, $k = 1.0$; for $T_1 \geqslant 2.5$ s, $k = 2.0$; and k is linearly interpolated between these values for 0.5 s $< T_1 < 2.5$ s. This is also recommended by design standards such as the International Building Code (IBC), USA. Some other design standards and guidelines, such as EC8 or ATC-40, suggested a distribution based on the fundamental mode shape (ϕ_1):

$$Q_i = V_d \frac{W_i \phi_{1i}}{\sum\limits_{i=1}^{n} W_i \phi_{1i}} \tag{13}$$

where ϕ_{1i} is the ith floor element in ϕ_1. The lateral load distribution determines the storey shear for each frame. For example, the distribution of storey shear (normalised to $V_d = 1.0$) for different lateral load distributions are shown in Fig. 13 for the eight-storey frame.

Values of R and its components considering lateral load distributions based on ASCE7 and the fundamental mode shape are shown in Tables 18 and 19, respectively. Other considerations in
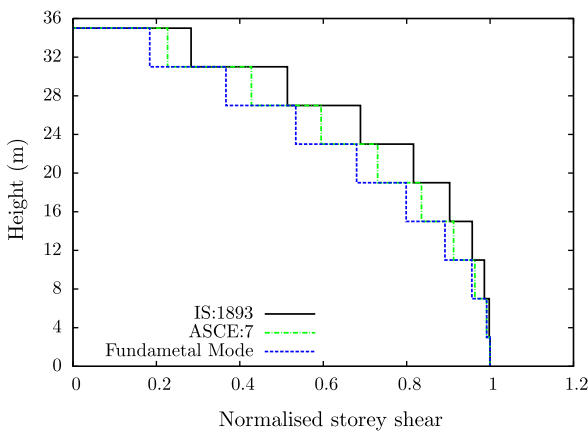
Fig. 13. Typical storey shear pattern of the eight-storey frame for different lateral load distributions.

Table 18
Components of R considering a lateral load distribution as per ASCE7.

Frame	Based on PL1				Based on PL2			
	R_s	R_μ	R_R	R	R_s	R_μ	R_R	R
2-storey	2.76	1.91	1.00	5.27	2.76	2.88	1.00	7.94
4-storey	2.63	1.73	1.00	4.56	2.63	2.35	1.00	6.18
8-storey	2.34	2.10	1.00	4.91	2.34	2.53	1.00	5.92
12-storey	2.20	2.11	1.00	4.64	2.20	3.00	1.00	6.00

Table 19
Components of R considering a lateral load distribution based on the fundamental mode shape.

Frame	Based on PL1				Based on PL2			
	R_s	R_μ	R_R	R	R_s	R_μ	R_R	R
2-storey	2.70	2.03	1.00	5.50	2.70		1.00	7.63
4-storey	2.64	2.01	1.00	5.31	2.64	2.32	1.00	6.14
8-storey	2.39	2.05	1.00	4.90	2.39	2.51	1.00	5.98
12-storey	2.26	2.08	1.00	4.70	2.26	2.83	1.00	6.39
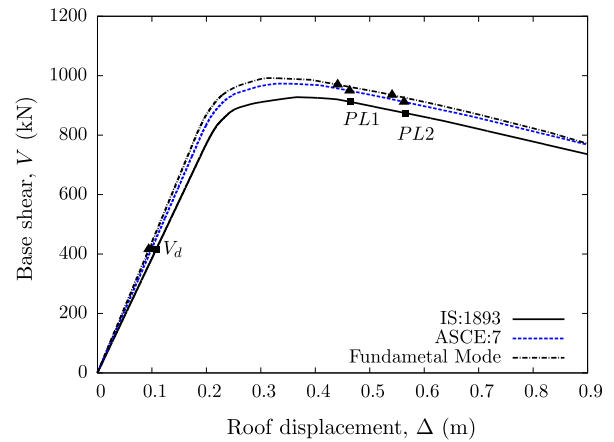
Fig. 14. Pushover curves for the eight-storey frame for different lateral load distributions.

these computations remain the same as in Sections 7.1 and 7.2. As shown in the sample pushover curves for the eight-storey frame (Fig. 14), the ultimate performance points are slightly affected by a change in the distribution of Q_i adopted in the NSPA. For PL1, the R values increase (from those based on the IS 1893 distribution) to the range of 4.56–5.27 for the ASCE7 distribution and to 4.70–5.50 for the ϕ_1-based distribution. For the ϕ_1-based distribution, both the ductility and strength factors increase, while it is only the strength factor increasing for the ASCE7 distribution. Similar changes are observed for PL2, both for R and its components, where R increases (except for the two-storey frame) to the ranges of 5.92–7.94 and 5.98–7.63, respectively.

8. Concluding remarks

A detailed study has been conducted to check the validity of the response reduction factor (R) value recommended in IS 1893 for 'ductile'/'special' RC moment resisting frames. The work presented here has considered four RC moment framed buildings, with fundamental vibration periods covering a large spectrum, located in zone IV and designed and detailed following the Indian standard guidelines IS 1893 and IS 13920. The focus has been in the following areas: a component-wise calculation of the factor R; consideration of realistic performance-based limit states at both structure and member levels; detailed modelling of the inelastic moment–curvature behaviour, P–M interaction, and plastic rotation capacity; and consideration of realistic design practices.

The major conclusions of the research presented here are

• Based on *Performance Limit 1* (ATC-40 limits on interstorey drift ratio and member rotation capacity), the Indian standard overestimates the R factor, which leads to the potentially dangerous underestimation of the design base shear.

- The actual value of R in real life designs is expected to be even lower than what is computed here, because of various reasons, such as, irregularity in dimensions leading to minor to moderate torsional effects, lack of quality control and poor workmanship during the construction, not following the ductile detailing requirements exactly as per the guidelines, etc.
- Based on *Performance Limit 2* (member rotation limits based on section dimensions and actual reinforcements), the IS 1893 recommendation is on the conservative side. It should however be noted that this limit does not include any structure level behaviour such as interstorey drift.
- The strong-column-weak-beam criterion in design does not make any major difference in terms of R.
- An accurate estimation of the fundamental period (T_1) is necessary for estimating a realistic R of a structure, specifically if T_1 is in the constant S_a zone of the design spectrum.
- R (for PL1) comes to be close to the IS 1893 recommended value if P–Δ effects are not considered. So, $R = 5.0$ may be safe for a design where P–Δ effects are actually negligible at the ultimate state.
- The IS 1893 and the ASCE7 lateral load distributions give R almost in the same range. However, a load distribution based on the fundamental mode shape estimates R in a range of higher values.

The conclusions of the present study are limited by the facts that only a single plan configuration (without plan-asymmetry) in one single seismic zone has been considered. In addition, the structural behaviour is not validated by any nonlinear response-/time-history analysis. The different parameters used in the work presented have been considered to be deterministic, although in reality their statistical variations are significant enough requiring a reliability-based framework for this study.

References

[1] ASCE SEI/ASCE 7-05. Minimum design loads for buildings and other structures. Reston (USA): American Society of Civil Engineers; 2005.
[2] CEN Eurocode 8. Design Provisions for earthquake resistance of structures (European Prestandard ENV 1998). Brussels (Belgium): Comité Européen de Normalisation; 2004.
[3] BIS IS 1893: Criteria for earthquake resistant design of structures, Part 1. New Delhi (India): Bureau of Indian Standards; 2002.
[4] BIS IS 456: Plain and reinforced concrete-code of practice. New Delhi (India): Bureau of Indian Standards; 2000.
[5] BIS IS 13920: Ductile detailing of reinforced concrete structures subjected to seismic forces-code of practice. New Delhi (India): Bureau of Indian Standards; 1993.
[6] Whittaker A, Hart G, Rojahn C. Seismic response modification factors. J Struct Eng, ASCE 1999;125(4):438–44.
[7] Kappos AJ. Evaluation of behaviour factors on the basis of ductility and overstrength studies. Eng Struct 1999;21(9):823–35.
[8] Borzi B, Elnashai AS. Refined force reduction factors for seismic design. Eng Struct 2000;22(10):1244–60.
[9] Newmark N, Hall W. Earthquake spectra and design. Engineering monograph; Earthquake Engineering Research Institute, Berkeley, California; 1982.
[10] Riddell R, Newmark N. Statistical analysis of the response of nonlinear systems subjected to earthquakes. Structural research series no. 468; Dept. of Civil Engineering, University of Illinois; Urbana, USA; 1979.
[11] Vidic T, Fajfar P, Fischinger M. A procedure for determining consistent inelastic design spectra. In: Nonlinear seismic analysis of reinforced concrete buildings, New York, USA; 1992.
[12] Krawinkler H, Nassar A. Seismic design based on ductility and cumulative damage demands and capacities. In: Nonlinear seismic analysis of reinforced concrete buildings, New York, USA; 1992. p. 27–47.
[13] Miranda E, Bertero V. Evaluation of strength reduction factors for earthquake-resistant design. Earthq Spectra 1994;10(2):357–79.
[14] ATC ATC-40: Seismic evaluation and retrofit of concrete building, vol. 1. Redwood City (USA): Applied Technology Council; 1996.
[15] FEMA Prestandard and commentary for the seismic rehabilitation of buildings (FEMA-356). Washington (USA): Federal Emergency Management Agency; 2000.
[16] Kent D, Park R. Flexural mechanics with confined concrete. J Struct Div, ASCE 1971;97(ST7):1969–90.
[17] Mander J, Priestley M, Park R. Theoretical stress strain model for confined concrete. J Struct Eng, ASCE 1988;114(8):1804–26.
[18] Baker A, Amarakone A. Inelastic hyperstatic frames analysis. In: Proceedings of the international symposium on the flexural mechanics of reinforced concrete. Miami: ASCE-ACI; 1964. p. 85–142.
[19] Roy H, Sozen M. Ductility of concrete. In: Proceedings of the international symposium on the flexural mechanics of reinforced concrete. Miami: ASCE-ACI; 1964. p. 213–24.
[20] Soliman M, Yu C. The flexural stress-strain relationship of concrete confined by rectangular transverse reinforcement. Mag Concr Res 1967;19(61):223–38.
[21] Sargin M, Ghosh S, Handa V. Effects of lateral reinforcement upon the strength and deformation properties of concrete. Mag Concr Res 1971;23(75–76):99–110.
[22] Sheikh S, Uzumeri S. Strength and ductility of tied concrete columns. J Struct Eng, ASCE 1980;106(5):1079–102.
[23] Saatcioglu M, Razvi S. Strength and ductility of confined concrete. J Struct Eng, ASCE 1992;118(6):1590–607.
[24] Sharma A, Reddy G, Vaze K, Ghosh A, Kushwaha H. Experimental investigations and evaluation of strength and deflections of reinforced concrete beam column joints using nonlinaer static analysis. Technical report; Bhabha Atomic Research Centre; Mumbai, India; 2009.
[25] Priestley M. Displacement-based seismic assessment of reinforced concrete buildings. J Earthq Eng 1997;1(1):157–92.
[26] Park R, Paulay T. Reinforced concrete structures. New York (USA): John Wiley & Sons; 1975.
[27] Prakash V, Powell GH, Campbell S. DRAIN-2DX, base program description and user guide: version 1.10. Report no. UCB/SEMM-93/17; University of California, Berkeley, USA; 1993.
[28] Prasanth T, Ghosh S, Collins KR. Estimation of hysteretic energy demand using concepts of modal pushover analysis. Earthq Eng Struct Dynam 2008;37(6):975–90.
[29] Ghosh S, Datta D, Katakdhond AA. Estimation of the Park–Ang damage index for planar multi-storey frames using equivalent single-degree systems. Eng Struct 2011;33(9):2509–24.
[30] Chryssanthopoulos MK, Dymiotis C, Kappos AJ. Probabilistic evaluation of behaviour factors in EC8-designed R/C frames. Eng Struct 2000;22(8):1028–41.